Prototype design of an aerial robotic platform for indoor applications

Natasha Botha[1*], *Beatrice* van Eden[1], *Lodewyk* Lehman[1], and *Jaco* Verster[1]

[1]Centre for Robotics and Future Production, Manufacturing Cluster, Council for Scientific and Industrial Research, South Africa

Abstract. There is an increased interest in using aerial robotic platforms for indoor applications in industrial and manufacturing environments. One such example is stocktaking in warehouses, where the use of other mobile robotic systems is not efficient as they aren't able to reach higher shelves or operate at the same speed as an aerial robotic platform. In this paper we discuss a prototype design for an aerial robotic platform that will be able to operate in GPS-denied areas, such as indoor warehouses. Suitable choices for the hardware and avionics are proposed based on the system and user requirements. The final design weighs 194 g, costs R 7 354.3, and has an estimated flight time of 5.5 min which is within the system requirements.

1 Introduction

In the industrial and manufacturing industries there is an increasing interest in the use of aerial robotics to increase the level of automation [1]. Aerial robots have an advantage over ground robots and humans as they are more agile and have a wide range of applications [2]. They can reach areas otherwise inaccessible and are often deployed in dangerous environments.

An ideal use case for aerial robots in an industrial and manufacturing setting is to provide automated stocktaking in a warehouse. Currently, stocktaking efforts in South Africa require the temporary employment of several additional people to assist. Using mobile robotic platforms is not efficient as these cannot access the higher shelves, even if a robotic arm is added to the platform. Aerial robotic platforms lean themselves to such a mundane task, able to perform more efficiently and reach the higher shelves easier than either a mobile robot or human. In addition, for indoor applications the GPS signal is often distorted and as a result commercial aerial robotic platforms struggle to localise due to the lack of a signal.

We propose considering a swarm of autonomous aerial robots to perform indoor stocktaking. A swarm of aerial robots can share information and therefore carry different payloads depending on the specific platform's assigned task. For swarms it is recommended to consider smaller aerial robots as they are safer for indoor use and will pose little risk to their human colleagues [2].

One popular nano aerial vehicle platform that has been considered for swarm related research is the Crazyflie 2.1 [2]. The Crazyflie is an open source, open hardware research

* Corresponding author: nbotha1@csir.co.za

platform that has been used extensively in several research activities. For example, autonomous swarm behaviour [2,3], autonomous mapping [4], developing of controllers [5] and obstacle detection [6]. The Crazyflie 2.1 weighs only 27 g with a battery, has a diagonal dimension of 92 mm and a flight time of 7 min [7]. It has a lot of onboard processing power with a 32-bit 168-MHz ARM microcontroller and is equipped with a low-latency/long-range radio and Bluetooth LE [7]. The small size leans itself towards indoor swarm robotics, is safe for operation around humans and able to survive crashes at a high-speed due to its low inertia [2]. The Crazyflie 2.1 has an extensive ecosystem of software and deck expansions to assist in any intended application [7].

Phang et al. [8] also presented a design for a micro aerial vehicle which has a take-off weight of 50 g, a diagonal dimension of 142.54 mm and a flight time of 8 min. Their design focussed on the optimisation of the mechanical parts by considering constraints regarding the weight and performance.

The Crazyflie 2.1 is perfect for the intended stock taking and swarm application, and relatively inexpensive at US$ 225, which is R 4329.78 at the current exchange rate, excluding delivery and customs fees. The platform developed by Phang et al. [8] is not available commercially and a research platform used purely for their own purposes. Even though Crazyflie 2.1 is a potential platform it might be too small especially if additional sensors are required as its maximum payload weight is 15 g, which would limit the type of sensors.

This paper therefore focussed on designing and developing a prototype aerial robotic platform which will ultimately be used for indoor swarm applications. The aerial robotic platform needs to conform to the following requirements:

- Locally designed, low-cost solution.
- Able to operate in GPS-denied environments.
- Able to perform stocktaking tasks autonomously.
- Within the size range of a nano to micro aerial vehicle.
- Safe, stable, reliable, and robust platform that can work in collaboration with other platforms and humans.

The contribution of this study is the micro aerial robotic platform design which specifically focussed on indoor applications and is therefore able to operate in GPS-denied environments. Even though there are many commercial platforms available, these are largely for outdoor applications, with few able to operate in GPS-denied environments or that are small enough for the swarm applications. This paper aims to summarise the relevant theoretical analysis and experimental tests required during the design of an indoor aerial platform.

2 Robotic Platform Design

In this section the system requirements and the process followed to select the different hardware and avionics components, as well as the design of the airframe, is discussed.

2.1 System Requirements

The Crazyflie 2.1 is often used as a research platform in literature. For this study, similar specifications are considered for the prototype design, albeit slightly larger than the Crazyflie 2.1. The Crazyflie 2.1 is defined as a nano quadcopter, whereas the prototype in this study will be a micro aerial vehicle. A micro aerial vehicle is defined to have a maximum dimension no greater than 15 cm, an approximate lift off weight of 100 g, a payload of 20 g, a maximum flight speed of 15 m/s, and flight endurance of 20 min [9,10]. The system requirements are developed by considering both the Crazyflie 2.1 and the definition of the micro aerial vehicle. The system requirements are summarised in Table 1.

Table 1. Overview of the system requirements.

Requirement	Crazyflie 2.1 [7]	Prototype
Diagonal Length (mm)	92 mm	150 – 200 mm
Weight (g)	27 g	100 – 200 g
Payload (g)	15 g	20 – 40 g
Flight time	7 min	< 20 min
Flight speed	1 m/s	< 15 m/s
Microcontroller	STM32F405 main application MCU (Cortex M4, 168 MHz, 192 kb SRAM, 1 Mb flash)	Flight and electronic speed controller with similar specifications. Onboard processing capabilities.
IMU	3 axis accelerometer/gyroscope	3 axis accelerometer/gyroscope
Cost	R 4 329.78 + R 602.21 shipping = R 4 931.99	< R7 000

2.2 Selection of Hardware Components

The core of any aerial robotic platform is its hardware and avionics. The most important component to select is the flight controller, responsible for ensuring stable and balanced flight operations. Other components include the motors, electronic speed controller, battery, propellers, receiver, transmitter, and sensors. The initial prototype design will only consider a camera as the main sensor which is considered part of the payload.

2.2.1 Motor and Propellers

The motor and propeller set of an aerial robotic platform is the main actuators. For a quadrotor configuration four sets of motos and propellers are required and need to be selected carefully to satisfy the system requirements [8]. In selecting a motor, it is necessary to consider the total revolutions per minute (rpm), operation voltage, current consumption, weight, maximum thrust, and cost [8]. The total rpm is calculated by considering the K_v rating and voltage of the motor:

$$rpm = \frac{K_v \times V}{2} \tag{1}$$

The total thrust required uses the total weight and a 2:1 power to weight ratio, which is ideal for standard control on aerial robots:

$$\begin{aligned} total\ thrust\ required &= w_{total} \times power{:}\,weight \\ &= 161.48 \times 2 \\ &= 322.96\ g \end{aligned} \tag{2}$$

To successfully ensure that the aerial platform can fly a total thrust of 322.96 g is required which is 80.74 g per motor.

The Crazyflie 2.1 uses DC coreless motors which have similar benefits to a brushless motor but do not last as long. A brushless motor provides better flight performance and durability, and don't require a lot of maintenance [11]. We identified three potential motors to consider for the prototype as shown in Table 2. The first row is a DC coreless motor similar to what Crazyflie 2.1 uses, the other two are brushless motors often recommended for first person view (FPV) aerial platforms.

Table 2. Motor specifications.

Motor	K_v (rpm/V)	Voltage (V)	Max Current (A)	rpm	Thrust (g)	Weigh t (g)	Cost (R)
CMU Coreless Micro DC	11 428 K_v	3.5 V	0.1 A	20 000 rpm	15 g	3 g	R 30
Racestar BR1103B	8000 K_v	11.7 V	4.7 A	14 800 rpm	78 g	3.7 g	R 535
T-Motor F1303	5000 K_v	11.7 V	7.45 A	9 250 rpm	177 g	6.1 g	R 310

The BR1103B motor thrust was tested with a two-bladed propeller and the T-motor F1303 with a three-bladed propeller. The DC coreless motor and the BR1103B do not provide enough thrust per motor for the 80.74 g required. The T-motor F1303 can generate around 1.86 times the thrust required and is therefore selected as the motor for the prototype design. An added advantage is that the T-motor F1303 is described as silent and efficient, making a low-noise in an indoor environment.

A range of different two- and three-bladed polycarbonate propellers were considered as shown in Table 3. Note, these were selected based on the motor shaft diameter size, number of propellors, blade type and stock availability. As a result, we were only able to find one two-bladed option as larger two-bladed propellers were not in stock at the time of this study. We also purposefully selected a three-bladed propeller, Gemfan D63, which has a curved blade design compared to the straight bladed design of the other propellers.

Table 3. Propeller specifications.

Propeller	Nr of Blades	Shaft Diameter (mm)	Blade Diameter (mm)	Pitch	Weight (g)	Cost (R)
HQ Durable Prop T3 X 1.5	2	1.9 mm	76.2 mm (3 inch)	1.5	0.78 g	R 35
HQ Durable Prop T4 X 2	3	1.9 mm	101.6 mm (4 inch)	2	2 g	R 69
HQ Durable Prop T65 X 3	3	1.9 mm	65 mm	1.5	0.8 g	R 45
HQ Durable Prop T2.5 X 3.5	3	1.9 mm	63.5 mm (2.5 inch)	3.5	1.3 g	R 39
Gemfan D63	3	1.5 mm	63 mm	3	1.36 g	R 50

To select the most suitable propeller for the T-motor F1303 a thrust analysis was performed. This was done using a simple bench test which weighs the motor and propeller combination as it pushes down on a scale. The test setup is illustrated in Figure 1 where the flight controller was first connected to the ESC before connecting the motor. The components were then mounted on a piece of plywood to ensure everything is secure before placing it on an electronic scale. The tests were performed on a wooden table as soft surfaces can affect the readings. The flight controller is programmed via Betaflight where the rotational direction of the motor was set such that the generated force pushed the propeller down onto the scale to measure the applied thrust. It should be noted that in this configuration the airflow around the propellers can be affected due to a ground effect of blowing air straight onto the scale. This can potentially affect the thrust readings and will be investigated in future studies. The motor throttle was set in 10 % increments to generate the thrust and current curve, shown in Figure 2.

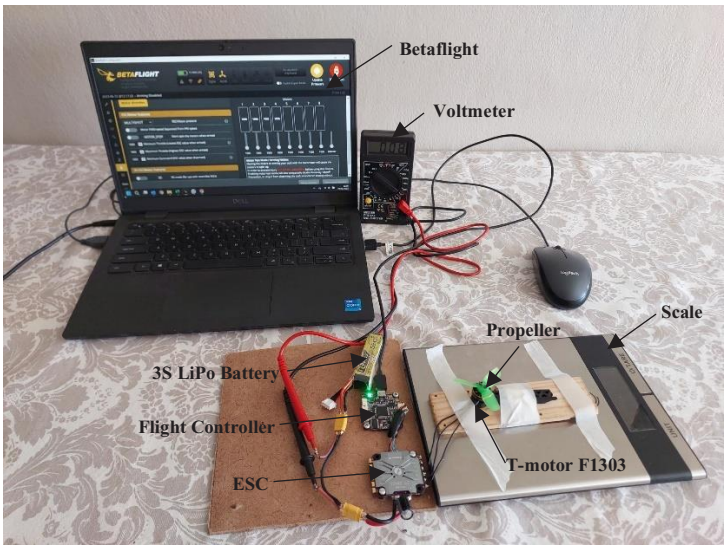

Fig. 1. Experimental bench test setup to determine the motor thrust

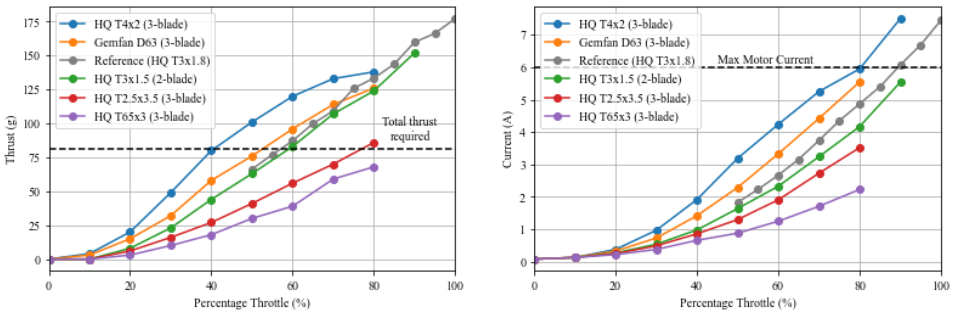

(a) Thrust (b) Current

Fig. 2. Percentage throttle versus thrust for different motor and propeller combinations

The dotted black line denotes the total thrust required in Figure 2(a) and the maximum allowable current the motor can withstand in Figure 2(b). Note the T-motor F1303 is indicated to have a maximum current of 7.45 A (Table 3) and the tests were done considering a 3 bladed HQ T3x1.8 prop [12]. The results from these tests are shown in grey as the reference propeller. Unfortunately, the same propellers could not be sourced and a few that are similar in size, although not exact, were therefore considered. The maximum motor current is selected as 6 A as the datasheet [12] indicates that the 7.45 A maximum current is only achievable for 60 s before the motor can no longer sustain it. This is why the percentage throttle is only up to 80 or 90 % of the maximum motor rpm to prevent motor burnout.

It is clear from Figure 2(a) that the HQ T4x2 (3-bladed), Gemfan D63 (3-bladed) and HQ T3x1.5 (2-bladed) are the only propellers that can meet the total thrust required. The HQ T3x1.5 (2-bladed) and Gemfan D63 propellers have similar thrust performances to the reference propeller used for the T-motor F1303 thrust tests. However, their current analysis is lower (HQ T3x1.5) and higher (Gemfan D63) compared to the reference, respectively. Overall, the HQ T4x2 (3-bladed) propeller provides the best performance achieving the thrust required at only 50 % of the motor throttle compared to 60 % for the Gemfan D63 (3-bladed) and HQ T3x1.5 (2-bladed). At these percentage throttles the current is just above 3 A, which is half of the maximum current the motor can sustain. Even though both 3-bladed propellers provide a better thrust this is at the expense of an increased current. Throughout the thrust tests these propellers required the motor to work much harder and therefore risk burnout. The HQ T3x1.5 (2-bladed) propeller does provide similar thrust performance to the reference propeller at a lower current. The HQ T3x1.5 (2-bladed) propeller is therefore selected for this design and the maximum motor throttle will be set to 70 % via Betaflight. This will assist in preventing motor burnout and thereby allowing for a longer flight time.

2.2.2 Flight Controller and Electronic Speed Controller

A flight controller is the computing centre of an aerial robotic platform. It sends information to the motors through the electronic speed controller (ESC) based on either the pilot's inputs through the remote control or flight controller software, or the computer program's inputs based on the output of mathematical algorithms [11]. Flight controllers also contain an inertial measurement unit (IMU) which is responsible for measuring the platform's motion, such as acceleration and angular rates, along 3-axes [8].

Phang et al. [8] and Crazyflie 2.1 opted to develop their own printed circuit board (PCB) which incorporates all the onboard electronics i.e., flight and electronic speed controllers. For the first iteration of the prototype, off the shelf commercial avionics that are, available locally were considered to ensure seamless integration of all the components. An additional requirement was to consider flight controllers that are compatible with the robot operating software (ROS) for future work. The flight controllers that were available locally are compared in Table 4.

Comparing the microcontrollers with the Crazyflie 2.1 (STM32F405) note that only the Matek F405-TE and Flycolor F4 have the same microcontrollers. The Pixhawk 4 mini's microcontroller provides more processing capacity than the other controllers, but it is very expensive and weighs almost 3 times than the Matek F405-TE and Flycolor F4. The ArduPilot APM 2.8 on the other hand has the lowest performing microcontroller and has a similar weight to the Pixhawk 4 Mini. All flight controllers have an appropriate IMU (a 3-axis gyro, accelerometer, and magnetometer) and use the same firmware and configuration interface. For the prototype design the Matek F405-TE is selected as it weighs less than the Flycolor F4 and has a barometer.

Table 4. Comparison of flight controllers.

Specification	ArduPilot APM 2.8	Pixhawk 4 Mini	Matek F405-TE	Flycolor F4
Micro-controller	**ATMEGA2560:** 8-bit AVR, 16 MHz CPU, 256 Kb flash memory, 8 Kb SRAM	**STM32F765:** 32-bit Arm Cortex-M7, 216MHz CPU, 2 Mb flash memory, 512 Kb SRAM	**STM32F405RGT6:** 32-bit Arm Cortex-M4 168 MHz CPU, 1 Mb flash memory, 192 Kb SRAM	**STM32F405:** 32-bit Arm Cortex-M4, 168 MHz CPU, 1 Mb flash memory, 192 Kb SRAM
IMU	MPU-6000	ICM-20689	ICM42688-P	MPU-6000
Barometer	MS5611-01BA03	MS5611	SPL06-001	No
Wi-Fi	No	No	No	No
Firmware	ArduPilot	ArduPilot	ArduPilot	OMNIBUSF4SD
Configuration Interface	Betaflight	Betaflight	Betaflight	Betaflight
ROS Compatibility	Yes	Yes	Yes	No
Weight	31 g	37.2 g	10 g	14.6 g
Cost	R 1 050	R 4 780	R 1 779	R 999

For the ESC the maximum current rating that it should be able to withstand to prevent the motors from overheating, is first determined [11,13]:

$$I_{ESC} = 1.2 \times I_{motor} = 1.2 \times 7.45 = 8.94\ A \quad (3)$$

There are two options to consider when selecting an ESC namely, to have a single ESC for each motor or a 4-in-1 controller. These are summarised in Table 5. Based on the current rating both options are suitable. Considering the single ESC, each motor would require one which would then have a total weight of 24.8 g and cost R 876. Even though it might cost less than the 4-in-1, the weight is a critical factor. For this reason, the Flycolor Trinx G5 60 A 4-in-1 ESC is selected for the prototype.

Table 5. Comparison of electronic speed controllers.

ESC Type	Component	Current	Battery	Weight	Cost
Single	Flycolor Raptor BLS Pro 30A Brushless	30 A	2 – 4S	6.2 g	R 219
4-in-1	Flycolor Trinx G5 60A	60 A	3 – 6S	19.6 g	R 1 699

2.2.3 Battery

The power supply of the aerial robotic platform needs to meet the overall system and flight duration requirements [8]. Generally, the power supply will contribute the most to the overall weight of the aerial robotic platform [8]. A Lithium-Polymer (LiPo) is the most popular choice of battery as they are lightweight and provide a high level of power. It should be noted that a higher capacity (mAh) also increases the battery weight. To successfully power the motors the battery voltage should match the motor voltage.

Considering the components already selected, the T-motor F1303 motors have a maximum voltage of 11.7 V and would require a 2 – 3S battery to power it, the flight controller requires a 3 – 8S battery and the ESC a 3 – 6S battery. A 3S battery is sufficient to power all the components. The only concern is the capacity which influences the flight time. The flight time is estimated using [14]:

$$t_{flight} = 60 \times \frac{P_{battery}}{I_{motor}} \tag{4}$$

Three LiPo 3S batteries with different capacities are compared in Table 6 and includes the estimated flight time calculated from Equation (4). Note that all three batteries have a nominal voltage of 11.1 V, which is comparable to the T-motor's maximum voltage of 11.7 V. The battery will therefore successfully power the motors. The Tattu batteries have a discharge rate of 95 C which indicates that current can be safely drawn from the battery 95 times more than the battery's capacity. To estimate the maximum flight time, it is assumed that the T-motor will not draw more than 6 A, as its peak current of 7.45 A can only be sustained for 60 s before the motor burns out. The estimated flight time might increase as the maximum throttle that the motor can reach will be set to 70 % via Betaflight, and the motor will therefore draw less current.

The CrazyFlie 2.1 has an estimated maximum flight time of 7 min, and the 750 mAh battery provides an estimated flight time close to this. The 2200 mAh battery on the other hand will provide an estimated maximum flight time of 22 min, which is closer to the system requirements (Table 1). However, this is achieved at the cost of weight, with this battery weighing 168 g i.e., 84 % of the maximum allowable weight of 200 g. That would leave only 32 g for all the other components, including the airframe. This would be impractical.

The 750 mAh battery would increase the platform weight to 205 g, only 5 g over the system requirements. This would require a total thrust of 102.5 g per motor which is still possible with the selected motor and propeller. The maximum motor throttle would just need to be changed to 60 % via Betaflight. There is a cost implication in selecting the larger battery, along with the increased weight.

For a first prototype the lighter and lower cost 550 mAh battery is selected and it will still provide a good flight time, especially with the motor throttle fixed at 70 %. In this case

it will also be comparable with the CrazyFlie 2.1 while retaining some weight and cost savings.

Table 6. Comparison of 3S batteries.

Battery	Discharge Rate	Capacity	Nominal Voltage	Maximum Continuous Current	Estimated Flight Time	Weight	Cost
Tattu R-Line 550 mAh	95 C	550 mAh	11.1 V	52.25 A	5.5 min	46 g	R 219
Tattu R-Line 750mAh	95 C	750 mAh	11.1 V	71.25 A	7.5 min	62 g	R 395
Gens ace Soaring 2200mAh	30 C	2200 mAh	11.1 V	66 A	22 min	168 g	R 360

2.2.4 Receiver and Transmitter

In order to manually control the aerial robotic platform a radio-frequency (RF) receiver is used to receive and decode the signals that are sent from a transmitter [8,11]. An aerial robotic platform is controlled by a qualified pilot in manual flight and should adhere to all rules and regulations of the regulatory body when flying outdoors, which in this case is the South African Civil Aviation Authority (SACAA). For indoor flight, there are no prescribed regulations, but a pilot should still operate as safely as possible. Most aerial robotic platforms are autonomous, such as Crazyflie 2.1 and the platform designed by Phang et al. [8], which doesn't require a receiver or transmitter, although it is common practice to retain the receiver as a fail-safe in case of emergencies where a pilot needs to take over [8]. For effective operations a 4-channel receiver is needed with a 900 MHz transceiver [11].

The long-term aim of the project is to navigate autonomously, the receiver and transmitter therefore needs to be cost-effective as it will not be a permanent feature for the prototype aerial robotic platform. The Flysky FS-i6X Transmitter with a iA6B Receiver was identified with an iA6B receiver that weighs 14.9 g, has 6 channels and a RF of 2.4 GHz, which is more than recommended.

2.2.5 Payload

An aerial robotic platform can consider any type of sensor as part of the payload, which is an additional allowable weight above the platforms total weight. These can include for example, GPS receivers, internal navigation systems, LiDAR (light detection and ranging) scanners, ultrasonic sensors, infrared cameras, thermal sensors, gas sensors, and visual cameras. These sensors allow for semi-autonomous or autonomous behaviour in addition to providing data to fulfil a certain task. For the prototype aerial robotic platform, the payload considered is a PC board for additional onboard processing capabilities and a camera sensor for visual navigation or perception.

A Raspberry Pi Zero with a 5 MP camera module weighing 15 g at a cost of R 660.80 was initially considered. However, due to the global electronics shortages we could not source one at the time of the study. As an alternative we selected an ESP32 with an OV5640 5 MP camera weighing 10 g at a cost of R 319.70 which is both lighter and more cost-effective than the Raspberry Pi.

2.3 Airframe Design

The airframe of an aerial robotic platform is the structure where all hardware components are mounted [11] The airframe should be light-weight and robust to accommodate the range of sensors and components while ensuring that the centre of gravity is evenly distributed.

For the prototype aerial robotic platform, the airframe was designed in the traditional cross configuration while considering 3D printing as the method of fabrication. The airframe, Figure 3, is designed in four parts: cross-frame, connectors, landing gear, and payload casing. The payload casing is not shown in this figure; however, it does connect at the hoop on the base of the landing gear.

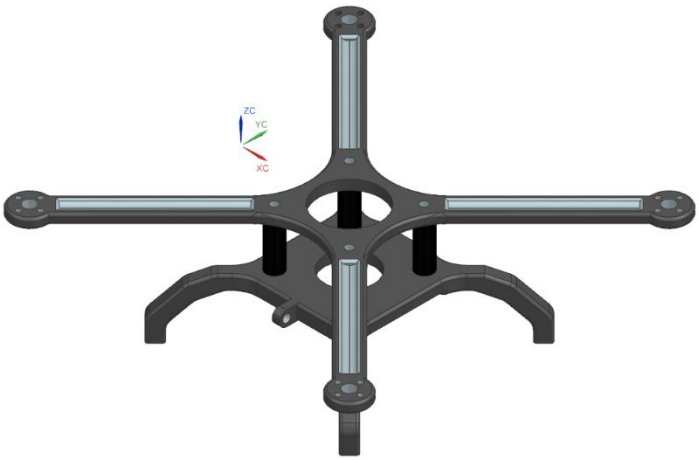

Fig. 3. Computer aided design (CAD) of the airframe.

The airframe has a diagonal dimension of 184 mm which is within the range of the system requirements, 130 mm between two motors mounting points, and a total height of 69 mm with the payload container and 55 mm without the payload container.

The frame was fabricated using polyethylene terephthalate glycol (PETG) which is a thermoplastic polyester commonly used in 3D printing applications due to is durability and strength. The Young's modulus for PETG is 3000 MPa with a yield strength of 53 MPa.

To reduce the weight and material needed the cross-frame thickness was determined by the length of the motor screws. In addition, slots were incorporated into the cross-frame for the motor's wires to run through. The frame was designed to be strong enough to support the payload yet flexible enough to absorb flight dynamics. To absorb the forces of a crash and minimise the risk of motor damage, the frame arms are intentionally designed to buckle and break upon impact.

The landing gear is solid, to assist in absorbing any impact should there be a hard landing or potential crash. The landing gear connectors have been designed to be approximately 1 mm shorter than the battery height. This design allows them to function as a clamp and secure the battery in place, allowing for final adjustments to the drone's center of gravity after all the components have been mounted.

Finite Element Analysis (FEA) was conducted on the drone frame to ascertain its structural integrity and the occurrence of excessive displacement under normal operational conditions. From a FEA simulation it is possible to identify areas of high stress or excessive deformation which are indicative of potential concerns or failures. This knowledge allows for design improvements to enhance the structural integrity of the airframe design.

Siemens NX was used to perform the FEA simulation with a three-dimensional mesh consisting of tetrahedral elements with a size of 2 mm. Fixed boundary conditions were applied at the four attachment points where the cross-frame connects to the landing gear with connectors. To replicate the thrust force exerted by the motors on the drone frame, a force of 177 g was applied in the centre of the location where the motor is connected (i.e., in the centre of each end point of the cross arm). The maximum thrust of 177 g used here is the maximum that the T-motor F1303 can achieve (Table 3). A constant gravitational load was incorporated to simulate the frame's response to gravity.

The results from the FEA simulation are provided in Figure 4 illustrating the total deflection of the cross-frame as well as Figure 5 showing the Von Mises stress. The maximum deflection of the cross-frame is 0.466 mm and the maximum Von Mises stress is 1.767 MPa. The maximum stress level remains significantly below the yield strength of the material (53 MPa) and there is no concern for a structural failure while flying the platform. Considering that the platform will operate at 70 % of its motor throttle, the forces encountered will be much lower than simulated. The airframe design is therefore sufficient with no failure anticipated during flight.

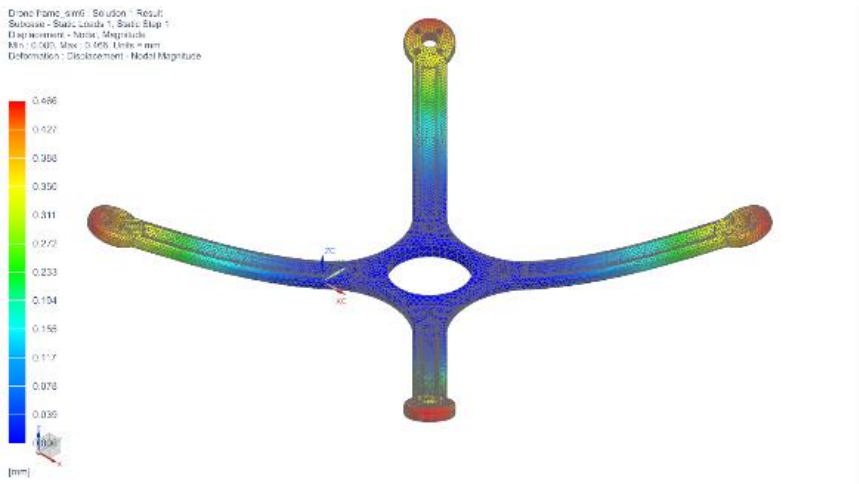

Fig. 4. Finite element analysis deflection results on the cross frame.

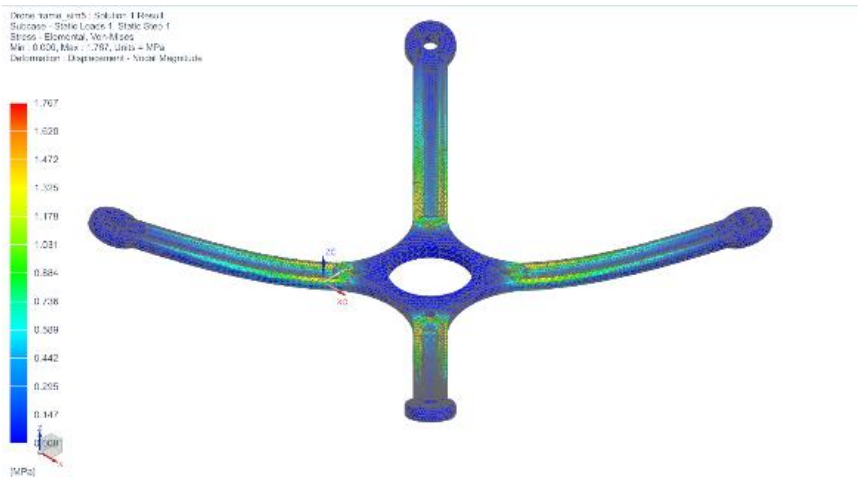

Fig. 5. Finite element analysis Von Mises stress results on the cross frame.

To improve upon the airframe design, optimisation methods, such as topology optimisation, can be considered to reduce the weight and material usage. To further optimise component placement a vibration analysis would also be beneficial for improved component placement.

3 Final Design

Table 7 provides a summary of the selected components and their associated weight and cost. All components were procured from local South African companies which are indicated as a footnote below the table.

Table 7. Summary of the final hardware specifications.

Component	Description	Weight	Unit Cost	Unit	Total Weight	Total Cost
Airframe	In-house design and 3D printed	36 g	R 350/kg	1	36 g	R 412.60*
Flight Controller[1]	Matek F405-TE	10 g	R 1 779	1	10 g	R 1 779
Electronic Speed Controller[1]	Flycolor Trinx G5 69A 4-in-1	19.6 g	R 1 699	1	19.6 g	R 1 699
Motor[2]	T-Motor F1303 KV5000	6.1 g	R 310	4	24.4 g	R 1 240
Battery[3]	Tattu R-Line 550 MAH 3S 95C	46 g	R 310	1	46 g	R 310
Propellers[1]	HQ Durable Prop T3x1.5 (2-bladed)	0.78 g	R 35	1	0.78 g	R 35
Receiver and Transmitter[1]	Flysky FS-i6X Transmitter with iA6B Receiver	14.9 g	R 1 559	1	14.9 g	R 1 559
Payload[4]	ESP32 with Camera OV5640	10 g	R 319.70	1	10 g	R 319.70
Total					**161.48 g**	**R 7 354.3**

***** To cover additional costs such as maintenance and electricity a R50 per hour printing time is allocated. The airframe took around 8 hours to complete which is R400.
[1] Flying Robot: https://flyingrobot.co/; [2] Boyz Toyz: https://boyztoyz.co.za/ ;
[3] Goblin Hobbies: https://www.goblinhobbies.co.za/ ; [4] Micro Robotics: https://www.robotics.org.za/

Comparing the total weight of 161.48 g to that of the system requirements (100 - 200 g) the prototype aerial robotic platform is within the weight range. This total weight was considered during the calculations to select an appropriate motor which will be able to lift the aerial robotic platform (Section 2.2.1). The final platform exact weight is 194 g, which is 32.52 g heavier than the estimated weight. This is mainly because of the connecting wires, and screws for mounting which wasn't accounted for in the estimated weight. From Equation (2) the thrust required for the exact weight is 97 g per motor which is achievable as the motor and propeller combination can produce a thrust of 107 g with the motors at 70 % throttle (see Figure 2).

The total cost of the aerial robotic platform is R 7 354.3 which is R 354.3 more than the intended maximum cost of R 7 000. The most expensive components are the flight controller, electronic speed controller and the receiver and transmitter. Note, the receiver and transmitter are a once-off cost and weight as future iterations of this prototype will be autonomous. It is therefore estimated that future iterations of the prototype will weigh 146.58 g and cost R 5 795.3 which is well within the system requirements. This lower cost is also closer to the cost of the CrazyFlie 2.1.

The final prototype aerial robotic platform is illustrated in Figure 6 considering the CAD model which will be used for future simulation-based studies, and the physical platform. The ESC and flight controller is mounted in the centre of the cross-frame and stacked on top of one another, while the battery is mounted between the cross frame and landing gear. The receiver is mounted in the slot beneath the landing gear and the ESP32 and camera in the payload container. A wiring diagram is provided in Figure 7 to illustrate the connections for all the electronic components.

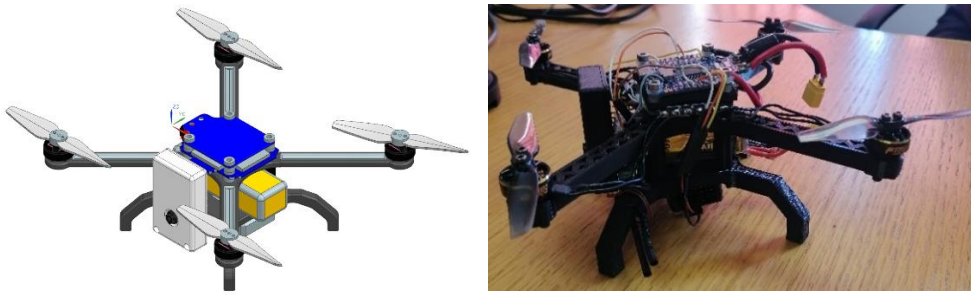

(a) CAD model (b) Physical platform

Fig. 6. Illustration of the prototype aerial robotic platform.

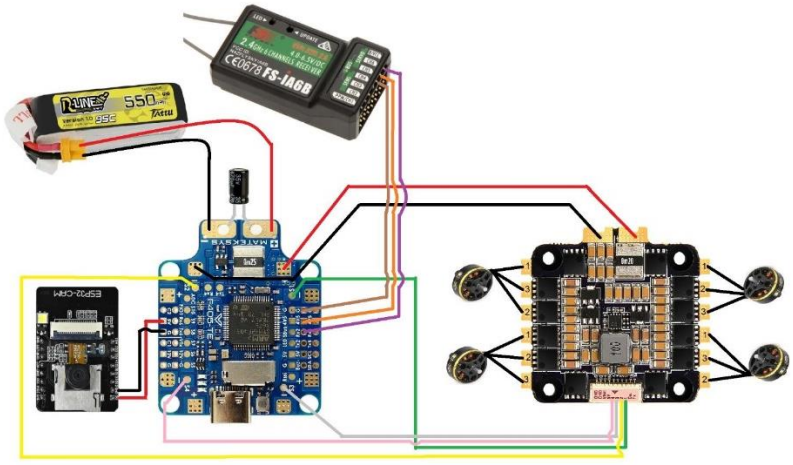

Fig. 7. Schematic of the wiring diagram for the hardware architecture.

Betaflight is used to set up the flight controller to ensure that it is not only safe to fly but that all motors are set up correctly. It is also necessary to initialise the transmitter (or remote controller) and bind it with the receiver before finalising the setup in Betaflight.

The aerial platform was flight tested a few times throughout development mainly to investigate the flight stability and the motor-propeller's ability to produce the thrust needed to lift the platform. In the initial flight tests the platform was able to fly with a fair amount of

stability albeit while drifting slightly in one direction. Another issue discovered during flight testing was that the motors tend to burn out when at full throttle. As explained during the thrust testing (Section 2.2.1) this is due to an increased current the motor cannot sustain. As a result, the motors were set to 70 % of the maximum throttle. Despite this, there is a persistent issue where the motors simply switch off even before 50 % of the motor throttle is applied.

Once this is resolved, a hover and manoeuvrability test will be performed using a Vicon motion capture system to quantify the platform's flight capability.

4 Conclusions

This paper presents a prototype aerial robotic platform to be used in industrial and manufacturing environments. The design of the platform conforms to the system and user requirements and follows a typical hardware architecture for a quadrotor design. Careful selection of the hardware components was made to ensure integration and the successful flight of the platform.

Due to unresolved hardware issues, it was not possible to quantify the aerial platforms flight capability. However, once these are resolved a hover and manoeuvrability test will be conducted using a Vicon motion capture system to quantify the performance.

Future iterations of the prototype will consider alternative potential components to reduce the overall weight and cost of the aerial robotic platform while increasing its performance. Based on the assembly there are a few recommended design changes to the airframe to improve mounting of the components and the overall aesthetic.

Future work will include the implementation of an autonomous flight capability, to remove the need for manual flight. For this a visual inertial odometry approach is considered using the onboard camera which has depth sensing to allow for safe navigation in confined spaces by avoiding obstacles. Also, designing and building a test frame which will allow for non-destructive flight testing, especially when starting with automated flight or testing different control algorithms.

The aerial robotics platform has the potential to be a great research platform in addition to being adopted in indoor (GPS-denied) industrial and manufacturing operations.

References

1. Perez-Grau, F.J., Martinez-de Dios, J.R., Paneque, J.L., Acevedo, J.J., Torres-Gonzalez, A., Viguria, A., Astorga, J.R., Ollero, A. 2021. Introducing autonomous aerial robots in industrial manufacturing, Journal of Manufacturing Systems, 60, pp. 312-324.
2. Preiss, J.A., Honig, W., Sukhatme, G.S., and Ayanian, N. 2017. Crazyswarm: A large nano-quadcopter swarm. IEEE International Conference on Robotics and Automation (ICRA), Singapore, pp. 3299-3304.
3. Duisterhof, B.P., Li, S., Burgues, J., Reddi, V.J., and de Croon, G.C.H.E. 2021. Sniffy Bug: A fully autonomous swarm of gas-seeking nano quadcopters in cluttered environments. Preprint arXiv: 2107.05490v1.
4. Mendes, K., Lemic, F., and Famaey, J. 2022. Small UAVs-supported autonomous generation of fine-grained 3D indoor radio environmental maps, IEEE International Conference on Distributed Computing Systems Workshops (ICDCSW), Bologna, Italy, pp. 296-301.

5. Lambert, N.O., Drew, D.S., and Yaconelli, J. 2019. Low level control of a quadrotor with deep model-based reinforcement learning, IEEE Robotics and Automation Letters, vol. 4(4), pp. 4224-4230.
6. Tayal, M., and Kolathaya, S. 2023. Control barrier functions in dynamic UAVs for kinematic obstacle avoidance: a collision cone approach. Preprint arXiv: 2303.15871v1.
7. Bitcraze AB (2023) Crazyflie 2.1. Available at https://www.bitcraze.io/products/crazyflie-2-1/. Last accessed on 24 May 2023.
8. Phang, S.K., Li, K., Chen, B.M., and Lee, T.H. 2015. Chapter 11: Systematic Design Methodology and Construction of Micro Aerial Quadrotor Vehicles, pp. 181-206. Handbook of Unmanned Vehicles. K.P. Valavanis, G.J. Vachtsevanos (eds.).
9. Cai, G., Dias, J., and Seneviratne, L. 2014. A survey of small-scale unmanned aerial vehicles: recent advances and future development trends, Unmanned Systems, vol. 2(2), pp. 1 – 26.
10. Pines, D.J., and Bohorquez, F. 2006. Challenges facing future micro-air-vehicle development, Journal of Aircraft, vol. 43(2), pp. 290 – 305.
11. Muruga Lal Jeyan, J.V., and Sreekumar, A. 2020. Methodical study of micro air vehicle/UAV device and its mechanism, AIP Conference Proceedings, vol. 2311, pp. 040017(1-11).
12. T-motor. (2023) F1303. Available on: https://store.tmotor.com/goods-1074-F1303.html. Last Accessed: 23 June 2023.
13. Saheb, S.H., and Babu, G.S. 2017. Design and analysis of light weight agriculture robot, Global Journal of Researchers in Engineering: A Mechanical and Mechanics Engineering, vol. 17(6), pp. 23-40.
14. Marode, S.T., Kale, P.C., and Lakal, N.V. 2014. Design, fabrication and testing of quadrotor prototype, International Journal of Engineering and Technical Research, vol. 2(5), pp. 97 – 103.